PRAMANA
— journal of
physics

Vol. 65, No. 4
October 2005
pp. 681–697

Synthesis and characterization of water-soluble carbon nanotubes from mustard soot

PRASHANT DUBEY, DEVARAJAN MUTHUKUMARAN, SUBHASHIS DASH, RUPA MUKHOPADHYAY and SABYASACHI SARKAR*
Department of Chemistry, Indian Institute of Technology, Kanpur 208 016, India
*Corresponding author. E-mail: abya@iitk.ac.in; jamtara@gmail.com

Abstract. Carbon nanotubes (CNT) has been synthesized by pyrolysing mustard oil using an oil lamp. It was made water-soluble (wsCNT) through oxidative treatment by dilute nitric acid and was characterized by SEM, AFM, XRD, Raman and FTIR spectroscopy. The synthesized wsCNT showed the presence of several junctions and defects in it. The presence of curved graphene structure (sp^2) with frequent sp^3 hybridized carbon is found to be responsible for the observed defects. These defects along with the presence of di- and tri-podal junctions showed interesting magnetic properties of carbon radicals formed by spin frustration. This trapped carbon radical showed ESR signal in aqueous solution and was very stable even under drastic treatment by strong oxidizing or reducing agents. Oxidative acid treatment of CNT introduced several carboxylic acid group functionalities in wsCNT along with the nicking of the CNT at different lengths with varied molecular weight. To evaluate molecular weights of these wsCNTs, an innovative method like gel electrophoresis using high molecular weight DNA as marker was introduced.

Keywords. Water-soluble carbon nanotubes; mustard soot; functionalization with hydrophilic groups; multipodal junctions; gel electrophoresis; molecular weight of wsCNT.

PACS No. 81.07.De

1. Introduction

Carbon nanotubes have been extensively studied over the past few years due to their unique structural features, amazing properties and for potential technological applications [1–18]. Several methods such as electric arc discharge in the absence or presence of metal [19,20], pyrolysis of hydrocarbons over catalyst [21], laser vaporization of graphite–metal composite target [22], electrolysis of metal salts with graphite electrodes [23] and hydrothermal methods [24] have been devised for the synthesis of multi-wall carbon nanotube (MWCNT) and single-wall carbon nanotube (SWCNT). With the high prospect of the potential use of CNT, its low-cost synthesis is highly desirable. Another important aspect of CNT is the development of its chemistry to improve its hydrophilic property whereby it could be solubilized in water. With the advancement of medical science, the role of water-soluble CNT in relevance to biotechnology is paramount [25]. The curious '*graphitic acid*' from

Bordie [26] has long been known to be essentially graphitic carbon possessing peripheral carbons in the form of oxidized carboxylic acid. Strong acids on prolonged reaction finally oxidize all forms of carbon to CO_2. In recent times, concentrated nitric acid (68%) treatment has been introduced to open up the ends of CNT [27]. Dilute nitric acid (2.6 M) washing treatment has been made to single-walled CNT to free it from metal catalyst and amorphous carbon [28]. Liu and co-workers [29] have used concentrated nitric acid-treated insoluble part of CNT, which apparently contained few surfacial carboxylic acid groups. Rao and co-workers [30] have synthesized water-soluble carbon nanotubes containing high proportion of acidic functional groups by refluxing multi-walled carbon nanotubes with H_2SO_4–HNO_3 (3 : 2 by volume).

Herein, we report a novel low-cost synthetic route to produce CNT by a simple and age-old method of burning of vegetable oil to prepare fresh carbon soot called *'kaajal'*. Synthesis of kaajal is long known and its use is even mentioned in epics like the *Ramayana* and the *Mahabharata*. This kaajal on oxidative treatment resulted in the synthesis of water-soluble carbon nanotube (wsCNT). These wsCNTs were structurally characterized by scanning electron microscopy (SEM) and atomic force microscopy (AFM). The XRD, Raman, FTIR, UV–Vis–NIR, fluorescence, EPR, and magnetic properties of these wsCNT were presented and a method, gel electrophoresis, is introduced with high molecular weight DNA as marker to separate the mixture of wsCNT.

2. Experimental details

2.1 *Synthesis and solubilization of carbon nanotube*

The mustard oil used in the experiment was procured from a local market and of edible quality. Normally vegetable oils contain glycerides of a mixture of several types of fatty acids. Mustard oil is comprised of 76% monosaturated, 23% polyunstaturated and 1% saturated fatty acids like oleic, linoleic, linolenic acids (all 18-carbon chain with unsaturation) and arachidic acid (20-carbon chain, saturated). Burning of other edible oils do produce soot of interesting properties (under investigation), but mustard oil was selected first because it contained very high unsaturated fatty acids among all the available, commonly used edible oils, and for its low cost. The raw soot was collected by burning mustard oil with the aid of a cotton piece in insufficient air. This soot is classically known as '*kaajal*' and has been in use as a medicament against common eye ailments and also as eye-liners. The temperature of the formation of this carbon soot from the burning of mustard oil was measured using a thermocouple (K-type, nickel–chromium–alumina). The soot was collected using a stainless steel collector from the top portion of the flame, where the temperature was around 650°C. The soot was placed in a thimble and sequential purification was performed using soxhlet extraction first by petroleum–ether followed by toluene, alcohol and finally by water to remove any unburnt oil and other soluble impurities. Finally the left out soot was air-dried. Such purified soot (1.0 g) was refluxed in an aqueous solution of HNO_3 (2.6 M, 200 ml) for 48 h. A good proportion of the soot went into the solution. The undissolved residue was

separated by centrifugation and the centrifugate was evaporated to dryness on a water bath to yield a black solid. Residual nitrate present in the solid was removed by repeatedly dissolving it in water and evaporating to dryness to finally yield a nitrate-free (tested by Griess's reagent [31]) black solid. Further purification was done by repeatedly dissolving it in water and reprecipitating it by adding alcohol. An alcohol soluble fraction of low molecular weight in the range 300–1400 D (checked by Maldi-Tof) was thus removed from the final water-soluble soot. Finally the black solid was repeatedly dissolved in water and evaporated to dryness to remove trace quantities of alcohol (tested by FT-IR) to yield 0.30 g of pure solid. This black solid is highly soluble (20 mg/ml) in water.

2.2 *Characterization of wsCNT*

The morphology and microstructure of wsCNT have been investigated using electron microscopy. SEM images were obtained on Cu stubs at accelerating voltages of 1–2 kV at 2 mm working distance using a JEOL-JSM-840 scanning electron microscopy (SEM), equipped with EDAX capabilities.

Atomic force microscopy (AFM) images were recorded in tapping mode in air at resonant frequencies of 22–25 kHz with oscillating amplitudes of 10–100 nm using a Pico SPM (molecular imaging) equipment with an AFM scanner. Images were obtained by the dynamic force mode. This mode involves cantilever oscillation either by an acoustic signal (AAC mode) [32] or by a magnetic signal (MAC mode) [33], leading to an enhanced resolution and minimal damage to the samples. AFM images of wsCNT were adsorbed onto AP-mica substrate. All the imaging was carried out with Si tips (k = 1–5 N/m). Minimum processing limited to 'first-order flattening' and 'brightness contrast' was employed when necessary.

Powder X-ray diffraction (XRD) spectra were collected on a Richseifert X-ray diffractometer (model Isodebyeflex 2002), operating in the Bragg configuration using CuK_α radiation (λ = 1.5418 Å) and Ni filter. Parameters used for slit widths and accelerating voltage, as well as Savitzky–Golay smoothing algorithms, were identical for all the samples.

Raman measurements were performed using SPEX-1877E spectrometer equipped with a triple monochromator. A 5 W Ar^+ laser (λ = 514.5 nm) was used as an excitation source. The samples were taken in powdered form on a glass holder. Charge coupled detector (CCD) was used as the detector and data were processed with the subtraction of laser-induced background luminescence using a personal computer.

FTIR spectra of the wsCNT from mustard soot were recorded on a Bruker Fourier transform infrared spectrometer (Vector 22 model) working with a globar lamp source, a KBr beam splitter and DTGS/KBr detector. The spectra were recorded in the solid state in KBr pellets in the range 400–4000 cm^{-1} with a resolution of 4 cm^{-1} and employing 32 repetitive scans to obtain a good signal-to-noise ratio. The spectra were first subtracted for the KBr pellet baseline before recording.

UV–Vis–NIR spectra were recorded on a Perkin Elmer Lambda 900 NIR spectrophotometer using quartz cells with a 10 mm path length. Samples for UV–Vis–NIR were prepared by dissolving carbon nanotubes in water. The collected

spectrum was corrected to account for a background absorption of the appropriate solvent. UV/Vis integration time for all the spectra were 0.2 s. The data interval was also kept constant at 1.0 nm. The spectrum of wsCNT in water was recorded in the range of 200–1400 nm.

All the fluorescence data were obtained on a Perkin-Elmer LS50B luminescence spectrometer, equipped with a 450-W xenon source and configured with double monochromators for both emission and excitation, with a 1s integration time. The excitation wavelength used was 364 nm. Spectra were recorded for blank solvent (water), and for 0.005% (w/v) wsCNT. The influence of pH variation in the fluorescence pattern of water-soluble carbon nanotubes, were studied by adding different concentrations of acid and base.

Electron spin resonance (ESR) spectra were recorded on a Bruker-EMX ESR spectrometer at a typical microwave frequency of 9.8 GHz and using a microwave power of 0.200 mW. The modulation amplitude employed was 5 G and the time constant was 10 ms. For the measurements, powdered samples were placed into EPR Wilmad 5 mm o.d. quartz tubes centered into the rectangular cavity. Solution ESR spectrum was recorded using flat quartz cell setup. Spectra processing (numerical integration, digital filtering, baseline correction and parameter calculation) were performed using Bruker WIN-EPR and SimFonia Software.

3. Results and discussion

3.1 *Microscopy*

A low (figure 1a) and high magnification (figure 1b) SEM micrograph of wsCNT from the mustard soot clearly showed the presence of extensive networked tubular structure with different types of junctions and branching. EDAX analysis confirmed the presence of oxygen along with carbon in the derivatize soot (figure 1c).

At higher magnification, as shown in figures 2a–d, the presence of different types of junctions and branching were clearly visible. These micrographs showed the presence of several turns and bents of complex shapes, sometimes with longer slender tubes. At the end, the slender tube changed its outer diameter to an L-shaped junction (figure 2d), which is very similar to joining two pipes of different diameters. In figures 2e, f, relatively uncomplicated but bent tubes are visible. One can readily recognize several types of junctions present in these micrographs. Thus L-shaped (dipodal) and Y- or T-shaped (tripodal) junctions was recognized. These complex structures have a lot of structural defects. These defects were introduced by the chaotic synthetic conditions of these CNTs under insufficient oxygen, which were augmented by subsequent acid treatment.

3.1.1 *Atomic force microscopy.* A typical tapping mode AFM image of wsCNT is shown in figures 3 and 4. The diameter of the wsCNT was found to vary between 9–30 nm, which supported that they were multi-walled nanotubes. The longest of the observed nanotubes was almost 1 μm in length (figure 4b). The side-walls of the tubules showed the presence of defective sites (figure 3), thus corroborating the findings of SEM studies presented above. These defects were expected because of the introduction of several carboxylic acid group functionalities on the surface of

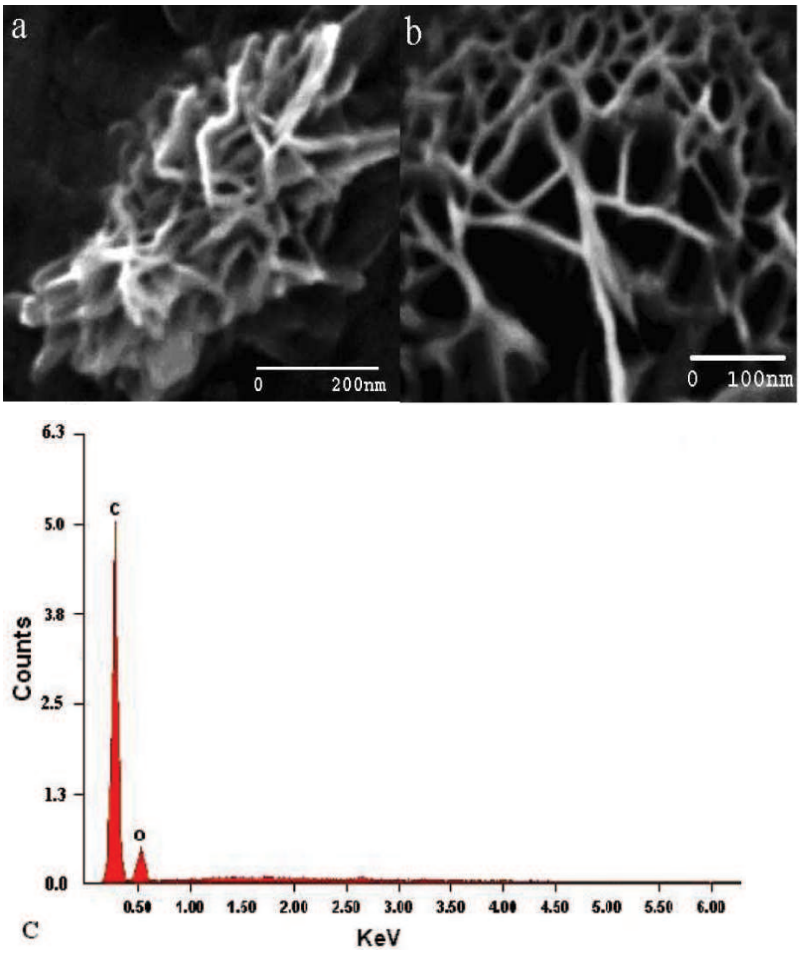

Figure 1. A low magnification (**a**) and high magnification (**b**) SEM image of wsCNT from mustard soot. (**c**) EDAX data (x-axis, keV and y-axis, counts.

the graphene sheet of the CNT. The introduction of sp^3 hybridization arising out of carboxylic acid function introduced defects. These might have been caused by the oxidation process, which introduced extensive functionalization on the side-walls of the nanotube.

3.2 *XRD study*

Figures 5a and b represented the XRD profiles of the soxhlet purified mustard soot and its derivative, wsCNT respectively.

Both the samples showed two predominant peaks. In the purified raw soot a high intense peak at 25.6 and a low intense peak at 44.0 were assigned for (0 0 2)

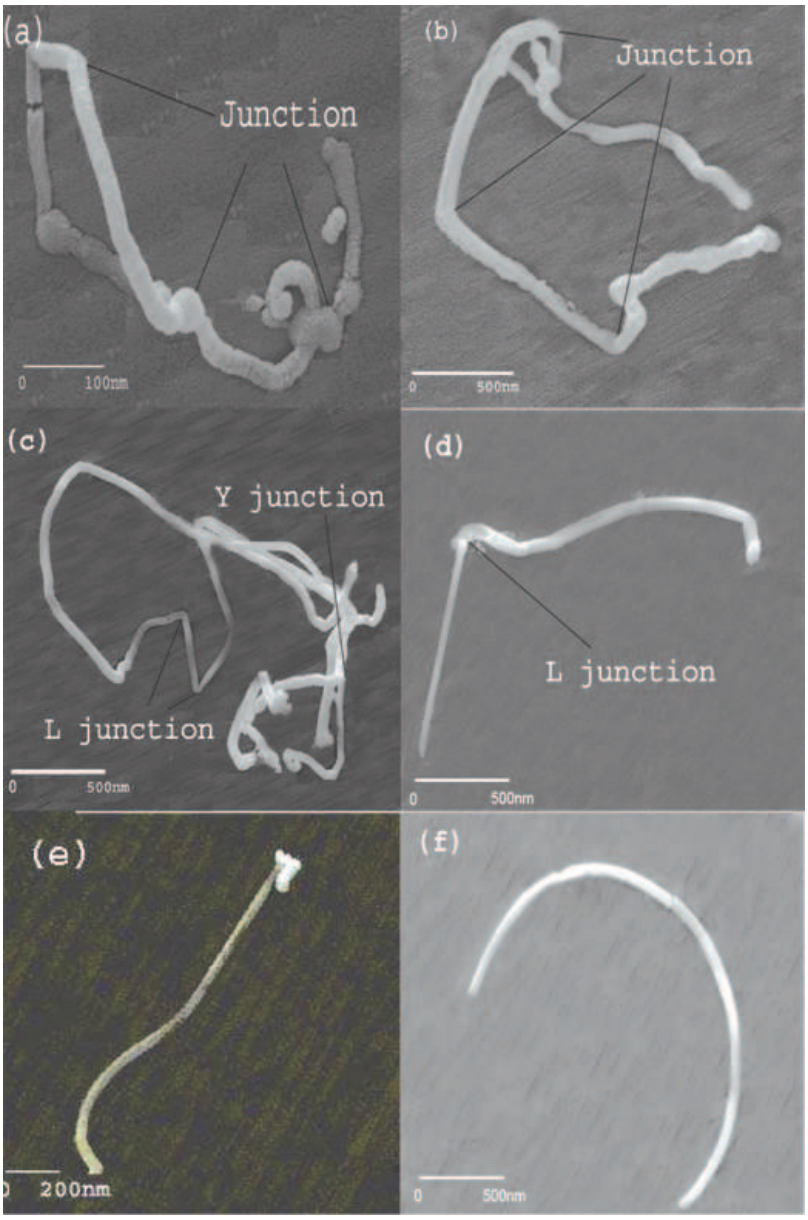

Figure 2. High magnification SEM image of wsCNT representing various bends and junctions.

and (1 0 0) reflections respectively. These reflections suggested that the tubules obtained by this method have good extent of graphitization. Similarly, in the case of wsCNT a high intense peak at 24.1 and low intense peak at 42.8 suggested that crystallinity is not lost due to oxidative acid treatment.

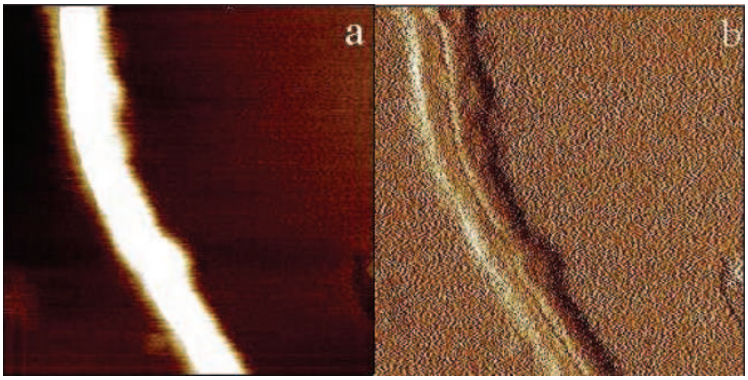

Figure 3a, b. AFM topograph of wsCNT from mustard soot (amplitude data: scan range = 80 × 80 nm; Z-range = 0–2 nm).

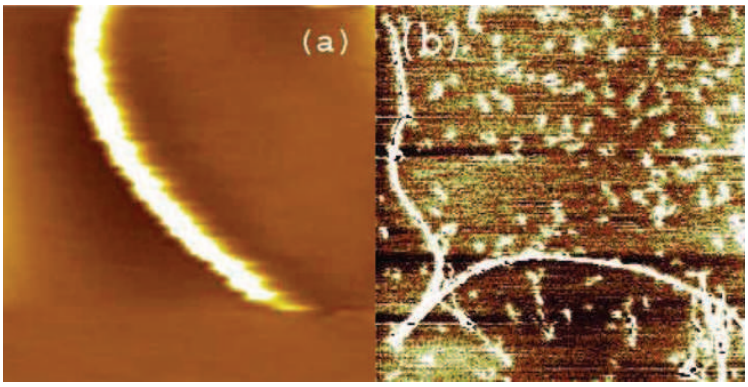

Figure 4. AFM topograph of wsCNT from mustard soot: (**a**) amplitude data: scan range = 100 × 100 nm; Z-range = 0–2 nm), (**b**) amplitude data: Scan range = 1000 × 1000 nm; Z-range = 0–2 nm) showing a long and branched carbon fiber.

3.3 *Raman study*

Raman spectra of soxhlet purified mustard soot and its wsCNT were shown in figures 6a and b respectively.

The Raman spectrum of soxhlet purified mustard soot has two prominent peaks at 1590 and 1347 cm^{-1} which corresponds to the E_{2g} (G-band) and disorder-induced (D-band) modes of graphite, respectively. The spectrum showed much wider bandwidth of the D-band compared to CNT obtained from graphite [34,35]. The similarity in the intensity of these two peaks was attributed to the presence of structural defects and more sp^3-hybridized carbon.

In the Raman spectrum of wsCNT, there were two prominent peaks at 1359 and 1612 cm^{-1} respectively. Both D-line and G-line have been down-shifted after oxidative treatment, but still both were of similar intensity as those of the raw soot with slight increase of G-line intensity. It is known that the D-line corresponds to

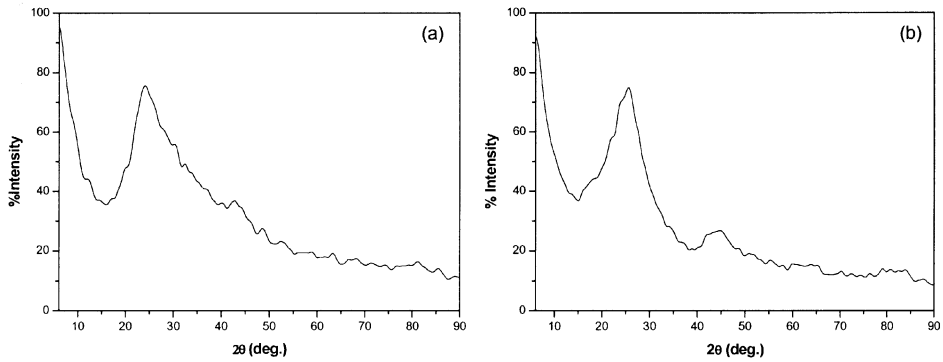

Figure 5. XRD pattern of (**a**) soxhlet purified mustard soot and (**b**) wsCNT from mustard soot.

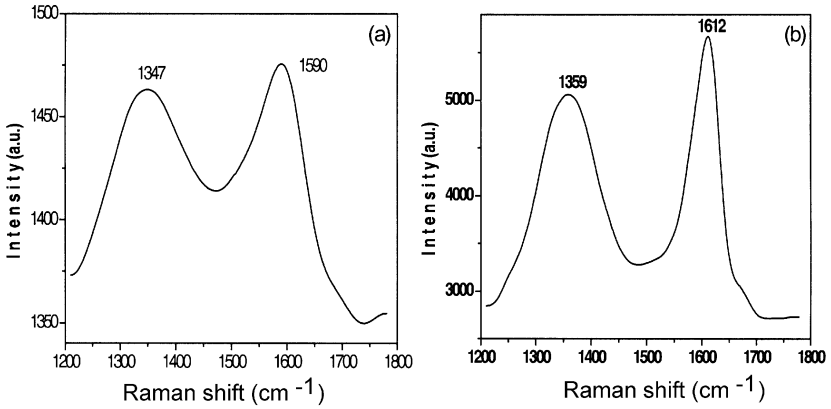

Figure 6. Raman spectra (laser wavelength = 514.5 nm) of (**a**) soxhlet purified mustard soot and (**b**) wsCNT from mustard soot.

stretching vibrations of sp^2-hybridized carbon atoms and the G-line is associated with disorder-induced symmetry-lowering effects [36]. Generally, functionalized carbon nanotube showed a decrease in the intensity of the G-line compared to the unfunctionalized carbon nanotubes [37]. The increase in the intensity of the D-line also indicated the structural deformation in the tube wall after the treatment with HNO_3 [38]. No peaks were observed in the lower wavelength region, and this could be due to the larger diameter of these tubules, as carbon nanotubes with diameters larger than 2 nm normally do not exhibit any peaks in the radial breathing mode (RBM) [39].

3.4 *FTIR study*

Infrared spectral data were used to study the carboxylic group functionalization of wsCNT. In figures 7a and b, FTIR spectra of soxhlet purified mustard soot and of the wsCNT were reproduced in the range 400–4000 cm^{-1}.

Figure 7a is a typical IR spectrum of soxhlet purified mustard soot, which was a carbon-based material with the absence of any absorption in the range 400–4000 cm^{-1}. For wsCNT (figure 7b), a band at 1725 cm^{-1} is attributed to (C=O) stretching vibration associated with the presence of carboxylic acid group. A broadband centered at 3436 cm^{-1} is assigned due to the (O–H) stretching vibration of the carboxylic acid group. A band centered at 1599 cm^{-1} and a shoulder at 1350 cm^{-1} may be due to (C=C) stretching vibrations. A band at ∼1217 cm^{-1} is associated with (C–O) stretching vibrations [40]. So the IR study directly prove the presence of carboxylic acid groups in wsCNT which corroborate the SEM, AFM and Raman results about the cause of structural defects in wsCNT. In an earlier study, [29] though the presence of surfacial carboxylic acid group was shown in CNT, that remained insoluble in water. At this stage it may be stated that the incorporation

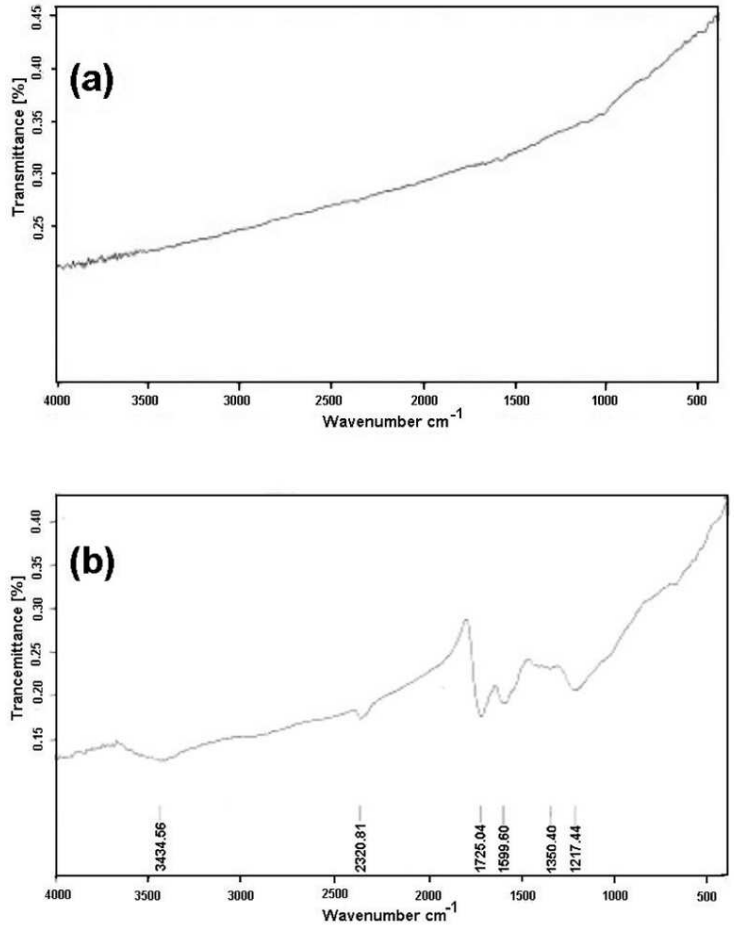

Figure 7. Infrared spectra of (**a**) soxhlet purified mustard soot and (**b**) wsCNT from mustard soot (in KBr).

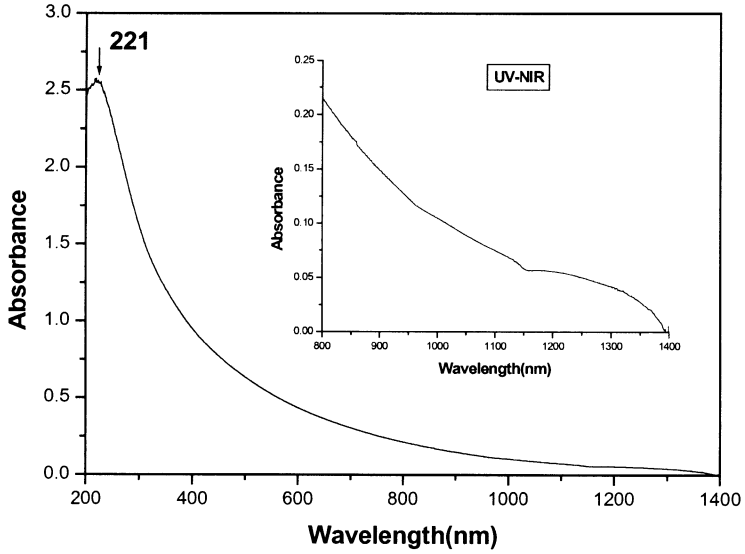

Figure 8. Electronic absorption spectrum of wsCNT from mustard soot in water.

of sufficient number of carboxylic acid groups per unit area in CNT may transform its hydrophobic property (insolubility in water) into hydrophilic nature resulting in its ready solubility in the form of wsCNT. The carboxylic acid groups may be present on the walls of the tubes and on the cap region of the tubes.

3.5 *Electronic spectral studies*

The electronic absorption spectrum of wsCNT from mustard soot in water was presented in figure 8.

The continuous increase in absorption in the range 1400 to 200 nm may be due to the overlap between the electrons of several double bonds and several carbonyl groups of the attached carboxylic acids. The optical characteristics of the sample monitored by absorbance at 400 nm and 500 nm have been found to obey Beer's law with respect to its relative concentration.

3.6 *Fluorescence study*

The fluorescence emission spectra of wsCNT from mustard soot in water upon excitation at 364 nm were shown in figure 9.

Strong luminescence at room temperature has been previously detected in nanotube solutions [41]. Here, in our system, the origin of this luminescence has been tentatively attributed to the existence of extensive conjugated electronic structures and excitation-energy trapping associated with defects in the nanotubes. Our

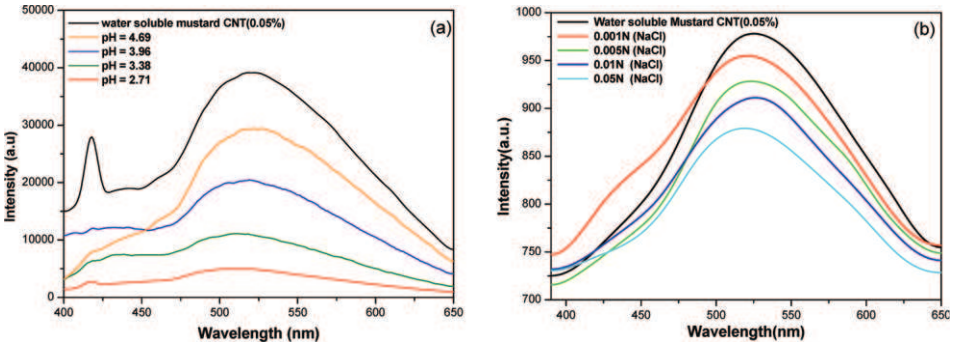

Figure 9. (**a**) pH-dependent fluorescence emission spectra of wsCNT from mustard soot in water at 364 nm excitation wavelength and, (**b**) ionic strength variation.

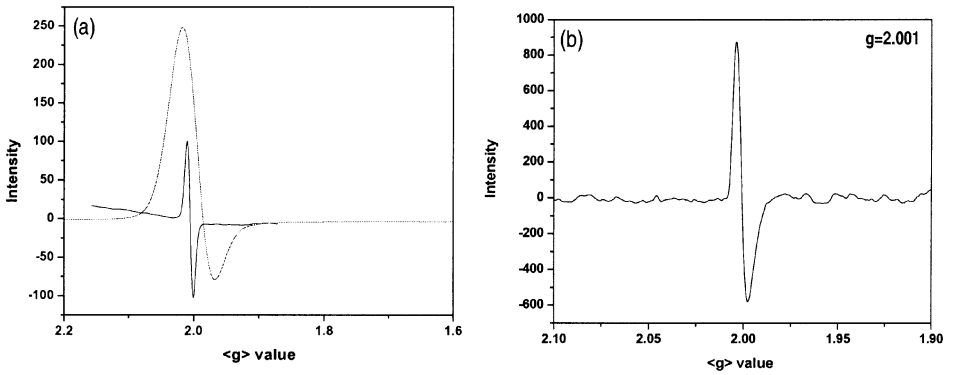

Figure 10. (**a**) Combined room temperature ESR spectra of soxhlet purified mustard soot (black), and wsCNT (red). (**b**) Aqueous solution ESR spectra of wsCNT.

luminescence studies in water indicated that the emission spectrum is dependent on pH (figure 9a) and on the ionic strength of the sample solution (figure 9b).

3.7 *ESR study*

Solid-state ESR spectra of soxhlet purified mustard soot and of wsCNT at room temperature were reproduced in figure 10a, which clearly indicated the presence of a stable carbon radical in mustard soot and also in wsCNT.

A dilute solution of wsCNT retained the ESR signal (figure 10b). Surprisingly this carbon radical was so stable that it could not be reduced or oxidized even by reagents like metallic Li or concentrated nitric acid respectively. The origin of the trapped carbon radical in a rigid graphene matrix is due to the presence of several junctions as discussed earlier. The negatively curved sp^2-bonded nano regions in the carbon structure [42] associated with multipodal junctions in wsCNT may cause spin frustration resulting in trapping of carbon radicals.

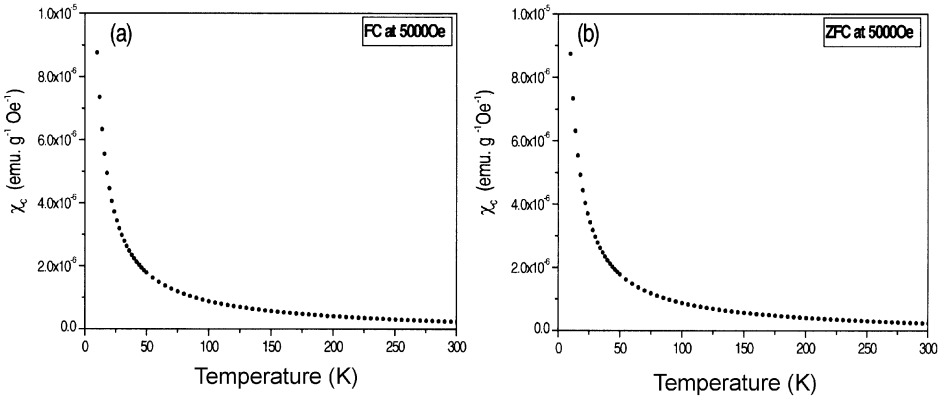

Figure 11a, b. Field-cooled (FC) and zero-field-cooled (ZFC) of χ_c vs. T plot at the field strength $H = 5$ kOe for wsCNT from mustard soot.

3.8 *Magnetic study*

In recent times, ferromagnetism has been reported in fullerene-based organic materials at low temperature [43–45] and even magnetism at room temperature has been observed in rhombohedral C_{60} [46]. It is well-known that CNT is diamagnetic in nature [47]. Theoretical predictions showed that pure carbon of sp^2 and sp^3 mixed phase can be responsible for ferromagnetic signal [48]. The magnetic measurements of wsCNT from mustard soot have been recorded in the 10–300 K temperature range by using powder sample in an inert atmosphere. The unusual temperature dependence of the dc magnetic susceptibility (χ_c) is shown in figure 11 at an applied magnetic field of 5 kOe. Unlike the value found for nearly all other forms of carbon, it showed a positive value. At room temperature (300 K), χ_c is equal to 2.5×10^{-7} emu·g^{-1} Oe^{-1}. It increased slightly with temperature and showed an upturn below 50 K. This behavior is directly related to the presence of unpaired electron in the system as has already been observed by ESR study.

The field dependence of the magnetization was also measured at temperatures 10, 25, 50 and 300 K (figure 12). The magnetic hysteresis in large magnetic field range (at 10 K and 300 K) is also shown (figure 13). A relatively small diamagnetic contribution due to straw and Teflon were subtracted from the original data. Our wsCNT from mustard soot showed characteristics of a soft magnet.

Such special and well-defined ferromagnetic behaviour of wsCNT has not been reported previously. With the increase in temperature, the magnetization value in the present case decreased while the magnetic state retained ferromagnetic loop up to room temperature. The value of magnetization depended on the outer diameter of the electron's spin orbit, which is fixed by the nanotube diameter and the number of layers present in the multi-walled wsCNT. This magnetic property of wsCNT can only be due to the presence of its intrinsic junctions and defective structures.

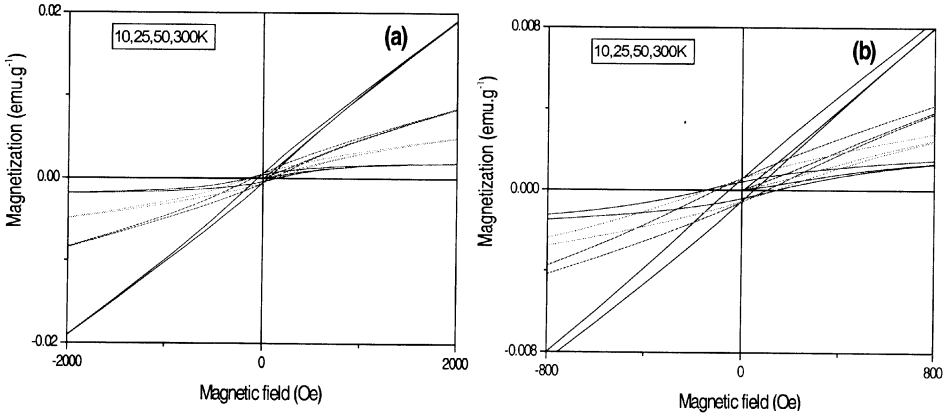

Figure 12. (**a**) Magnetic hysteresis loops for wsCNT from mustard soot at $T = 10$, 25, 50 and 300 K. **(b)** Enlarged part of the magnetization curve in the low-magnetic field region.

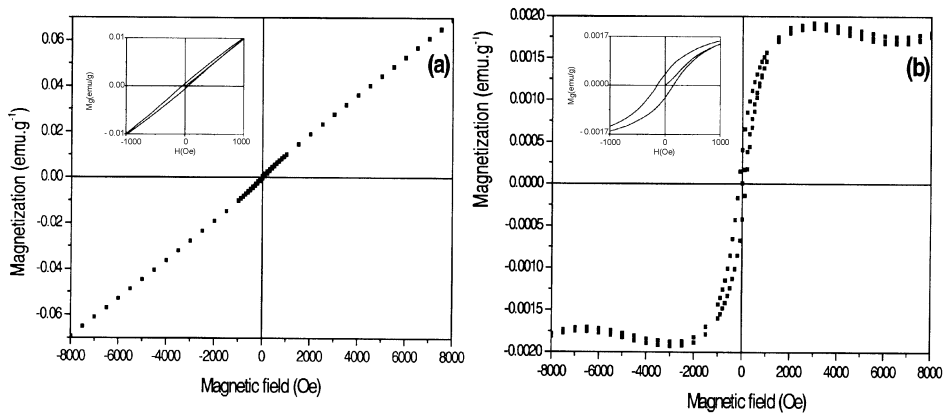

Figure 13. (**a**) Magnetic hysteresis loops for wsCNT from mustard soot at $T = 10$ K. Inset: enlarged part of magnetization curve in the low-magnetic field region. (**b**) Hysteresis loop for wsCNT from mustard soot at 300 K. Inset: enlarged part of the magnetization curve in the low-magnetic field region.

3.9 *Gel electrophoresis*

Significant advances in length and diameter separation of nanotubes have been made over the past few years [49,50]. Zheng and co-workers [51,52] have used a DNA (deoxyribonucleic acid) wrapping procedure followed by ion-exchange chromatography to yield nanotubes separated into fractions of narrow species distribution.

Due to the nicking of CNT by oxidative stress to form wsCNTs we could observe several types of shapes comprised of different lengths as seen in its SEM and AFM micrographs. Thus the wsCNT should comprise of several fractions with different molecular weights. We could use Maldi-Tof to note a distribution with mass

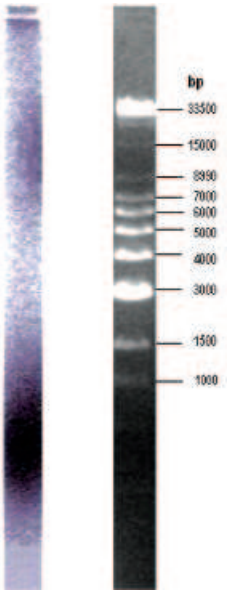

Figure 14. Agarose gel run for 30 min (40 V) containing wsCNT and super-mix DNA marker in a buffer of pH 8. Left lane: wsCNT and right lane: DNA with base pair (bp) marked.

around 50 kD. However, all these wsCNTs were heavily derivatized and were ionic in nature. This multi-ionic nature contributed varied m/z ratios thus thwarting to pin-point the real molecular weight. As the molecular weight of these fractions were very high and beyond the limit of any mass spectrometric technique including Maldi-Tof, we decided to use high molecular weight DNA as marker and to introduce gel electrophoresis for the separation of the mixture of wsCNT. The carboxylic acid group present in these wsCNTs are readily available in anionic form like the DNA. Using gel electrophoretic separation technique we could separate three bands out of the mixture of wsCNTs. Comparing their relative movements under identical conditions using super-mixed DNA (having very high base pairs) as molecular marker we could get a rough idea about the three bands of the separated wsCNTs. For the double-stranded DNA the average molecular weight of a unit of DNA with the pair of four nucleotides has unit molecular weight as 660 Da. Using 660 Da as the unit molecular weight of one base pair of a double-stranded DNA, the total base pairs present in a DNA band in gel electrophoresis would provide the idea about the molecular weight of DNA. When wsCNTs along with super-mix DNA (containg known DNA mixture with several base pairs) as molecular marker were subjected to gel electrophoresis (using TAE buffer, pH 8, and applied 40 V), three black bands from the wsCNT were identified. The bands from different base pairs containing super-mix DNA marker can be seen (under UV radiation) in the right lane (figure 14). Using such DNA bands as marker, our preliminary experiments provided the approximate molecular weight of these three bands ranging from 30 kDa, 990 kDa and the third one was much larger than 2211 kDa. With EDAX ratio obtained between oxygen and carbon and the relative intensity of Raman bands, a rough idea of the number of carboxylic acids present in a particular fraction of wsCNT with a resolved mass (separated by gel electrophoretic purification) may

be achieved. Thus the identification of a wsCNT fraction with its molecular weight and the number of its carboxylic acid content could be made and work is in progress in this direction.

4. Conclusion

We are able to show that '*kaajal*' made by burning mustard oil in a lamp actually contains CNT. The cause of its beneficial use for common eye ailments has not yet been known but may relate to its special structural property. This CNT can be readily derivatized and these derivatives do contain several junctions and other structural defects leading to bonding frustration of graphene carbons. CNT with defects contain trapped carbon radicals which have enormous stability. The discovery of magnetic carbon (present in wsCNT) in aqueous solution may open the door for future application as carbon-based spintronics .

Acknowledgements

Financial support for this work, from the 'Nanomaterials Science and Technology Initiatives Programme' of the Department of Science and Technology, New Delhi is gratefully acknowledged. Prashant Dubey thanks the Council of Scientific and Industrial Research (CSIR), New Delhi for a Senior Research Fellowship.

References

[1] T W Odom, J L Huang, P Kim and C M Lieber, *J. Phys. Chem.* **B104**, 2794 (2000)
[2] R H Baughman, A A Zakhidov and W A de Heer, *Science* **297**, 787 (2002); *Acc. Chem. Res. – Special Issue* **35**, 997 (2002)
[3] B S Sherigara, W Kutner and F D'Souza, *Electroanalysis* **15**, 753 (2003)
C N R Rao, B C Satishkumar, A Govindaraj and M Nath, *Chem. Phys. Chem* **2**, 78 (2001)
[4] S S Wong, J D Harper, P T Jr. Lansburry and C M Lieber, *J. Am. Chem. Soc.* **120**, 603 (1998)
[5] G Che, B B Lakshmi, E R Fisher and C R Martin, *Nature* **393**, 346 (1998)
[6] T Rueckes, K Kim, E Loselevich, G Tseng, C L Cheung and C M Lieber, *Science* **289**, 94 (2000)
A Bachtold, P Hadley, T Nakanishi and C Dekker, *Science* **294**, 1317 (2001)
M Bockrath, D H Cobden, P L McEuen, N G Chopra, A Zettl, A Thess and R E Smalley, *Science* **275**, 1922 (1997)
[7] H Ago, K Petritsch, M S P Shaffer, A H Windle and R H Friend, *Adv. Mater.* **11**, 1281 (1999)
[8] A Kasumov, R Deblock, M Kociak, B Reulet, H Bouchiat, I Khodos, Y Gorbatov, V Volkov, C Journet and M Burghard, *Science* **284**, 1508 (1999)
[9] R H Baughman, C Anvar, A Zakhidov, Z Iqbal, J N Barisci, G M Spinks, G C Wallace, A Mazzoldi, D De Rossi, A Rinzler, O Jaschinski, S Roth and M Kertesz, *Science* **284**, 1340 (1999)
[10] P Poncharal, Z Wang, D Ugarte and W Heer, *Science* **283**, 1513 (1999)

[11] C Niu, E Sichel, R Hoch, D Moy and H Tennet, *Appl. Phys. Lett.* **70**, 1480 (1997)
[12] S S Wong, E Joselevich, A T Woolley, C L Cheung, C M Lieber, *Nature* **394**, 52 (1998)
[13] J Kong, N Franklin, C Zhou, M Chapline, S Peng, K Cho and H Dai, *Science* **287**, 622 (2000)
[14] A Dillon, K Jones, T Bekkedahl, C Kiang, D Bethune and M Heben, *Nature* **386**, 377 (1997)
[15] P Calvert, *Nature* **357**, 365 (1992)
M S P Shaffer and A H Windle, *Adv. Mater.* **11**, 937 (1999)
[16] A Mamedov, N Kotov, M Prato, D Guldi, J Wisksted and A Hirsch, *Nat. Mater.* **1**, 190 (2002)
J Rouse, P T Lillehe, *Nano. Lett.* **3**, 59 (2003)
[17] P J Britto, K S V Santhanam, A Rubio, J A Alonso and P M Ajayan, *Adv. Mater.* **11**, 154 (1999)
C Downs, J Nugent, P M Ajayan, D J Duquette and K S V Santhanam, *Adv. Mater.* **11**, 1028 (1999)
[18] P M Ajayan and S Iijima, *Nature* **361**, 333 (1993)
L Ang, T Hor, G Hu, C Tung, S Zhao and J Wang, *Chem. Mater* **11**, 2115 (1999)
[19] S Iijima, *Nature* **354**, 56 (1991)
[20] S Iijima and T Ichihashi, *Nature* **363**, 603 (1993)
[21] T Guo, P Nikolaev, A Thess, D T Colbert and R E Smalley, *Chem. Phys. Lett.* **243**, 49 (1995)
[22] Y Gogotsia, J A Libera and M Yoshimura, *J. Mater. Res.* **15**, 2591 (2000)
[23] F Kokai, K Takahashi, M Yudasaka and S Iijima *J. Phys. Chem.* **B104**, 6777 (2000)
[24] W K Maser *et al*, *Chem. Phys. Lett.* **292**, 587 (1998)
W Wang, J Y Huang, D Z Wang and Z F Ren, *Carbon* **43**, 1317 (2005)
[25] J Chen, M A Hamon, H Hu, Y Chen, A M Rao, P C Eklund and R C Haddon, *Science* **282**, 95 (1998)
[26] N V Sidgwick, *The chemical elements and their compounds* (Clarendon Press, Oxford University Press, London, 1952) vol. I, p. 488
[27] S C Tsang, Y K Chen, P J F Harris and M L H Green *Nature* **372**, 159 (1994)
[28] J Liu *et al*, *Science* **280**, 1253 (1998)
A G Rinzler *et al*, *Appl. Phys.* **A67**, 29 (1998)
[29] L Liu, S Zhang, T Hu, T Guo, C Ye, L Dai and D Zhu, *Chem. Phys. Lett.* **359**, 191 (2002)
[30] C N R Rao, A Govindaraj and B C Satishkumar, *Chem. Commun.* 1525 (1996)
[31] P Griess, *Ber. Dtsch. Chem. Ges.* **12**, 427 (1879) as cited in Fiegl's spot tests in inorganic analysis (Elsevier, Amsterdam, 1958) p. 330
[32] P K Hansma, J P Cleveland, M Radmacher, D A Walters, P E Hillner, M Bezanilla, M Fritz, D Vie, H G Hansma, C B Prater, J Massie, L Fukunaga, J Gurley and V Elings, *Appl. Phys. Lett.* **64**, 1738 (1994)
[33] W Han, S M Lindsay and T Jing, *Appl. Phys. Lett.* **69**, 4111 (1996)
[34] J Kastner, T Pichler, H Kuzmany, S Curran, W Blau, D N Weldon, M Delamesiere, S Draper and H Zandbergen, *Chem. Phys. Lett.* **21**, 53 (1994)
[35] W S Bacsa, D Ugarte, A Châtelain and W A de Heer, *Phys. Rev.* **B50**, 15473 (1994)
[36] K Tanaka, T Yamabe and K Fukui, *The science and technology of carbon nanotubes* (Elsevier, Amsterdam, Lausanne, New York, Oxford, Shannon, Singapore, Tokyo, 1999)
[37] N I Kovtyukhova, T E Mallouk, L Pan and E C Dickey, *J. Am. Chem. Soc.* **125**, 9761 (2003)

[38] K H An, K K Jeon, J M Moon, S J Eum, C W Yang, G S Park, C Y Park and Y H Lee, *Synthetic Metals* **1**, 10379 (2003)
[39] S L Fang, A M Rao, P C Eklund, P Nikolaev, A G Rinzler and R E Smalley, *J. Mater. Res.* **13**, 2405 (1998)
[40] K Nakamoto, *Infrared and Raman spectra of inorganic and coordination compounds* 4th edition (John Wiley & Sons, New York, 1986)
[41] Y P Sun, B Zhou, K Henbest, K Fu, W Huang, Y Lin, S Taylor and D L Carroll, *Chem. Phys. Lett.* **351**, 349 (2002)
[42] N Park, M Yoon, S Berber, J Ihm, E Osawa and D Tom'anek, *Phys. Rev. Lett.* **91**, 237204 (2003)
[43] B Narymbetov *et al*, *Nature* **407**, 883 (2000)
[44] P M Allemand *et al*, *Science* **253**, 301 (1991)
[45] A Mrzel *et al*, *Chem. Phys. Lett.* **298**, 329 (1998)
[46] T L Makarova *et al*, *Nature* **413**, 716 (2001)
[47] R E Smalley *et al*, *Science* **265**, 84 (1994)
[48] A A Ovchinnikov and I L Shamovsky, *J. Mol. Struct. (Theochem.)* **83**, 133 (1991)
Yong-Hyun Kim *et al*, *Phys. Rev.* **B68**, 125420 (2003)
[49] S K Doorn, R E Fields, H Hu, M A Hamon, R C Haddon, J P Selegue and V Majidi, *J. Am. Chem. Soc.* **124**, 3169 (2002)
[50] D A Heller, R M Mayrhofer, S Baik, Y V Grinkova, M L Usrey and M S Strano, *J. Am. Chem. Soc.* **126**, 14567 (2004)
[51] M Zheng, A Jagota, E D Semke, B A Diner, R S Mclean, S R Lustig, R E Richardson and N G Tassi, *Nat. Mater.* **2**, 338 (2003)
[52] M Zheng, A Jagota, M S Strano, A P Santos, P Barone, S G Chou, B A Diner, M S Dresselhaus, R S McLean, G B Onoa, G G Samsonidze, E D Semke, M Usrey and D J Walls, *Science* **302**, 1545 (2003)